Disequilibrium melt distribution during static recrystallization

Nicolas P. Walte Tektonophysik, Institut für Geowissenschaften, Johannes Gutenberg-Universität Mainz, Germany
Paul D. Bons Institut für Geowissenschaften, Eberhard Karls Universität Tübingen, Germany
Cees W. Passchier, Daniel Koehn] Tektonophysik, Institut für Geowissenschaften, Johannes Gutenberg-Universität Mainz, Germany

ABSTRACT

Melt migration and segregation, and the rheology of partially molten rocks in the upper mantle and lower crust, strongly depend on the grain-scale distribution of the melt. Current theory for monomineralic aggregates predicts a perfectly regular melt framework, but high-temperature experiments with rock-forming minerals + melt show considerable deviations from this predicted geometry. Disequilibrium features, such as fully wetted grain boundaries and large melt patches, have been described; these were mainly attributed to surface-energy anisotropy of the minerals. We present static analogue experiments with norcamphor + ethanol that allow continuous in situ observation of the evolving liquid distribution. The experiments show that all previously reported disequilibrium features can form during fluid-enhanced static recrystallization when small grains are consumed. There is no need to invoke surface-energy anisotropy, although this might enhance the effect. All disequilibrium features are transitory and evolve back toward equilibrium geometry. However, because the system undergoes continuous static recrystallization, disequilibrium features are always present in a partially molten polycrystalline aggregate and therefore control its properties.

Keywords: analogue simulation, melts, porosity, permeability, norcamphor, recrystallization.

INTRODUCTION

Many properties of high-temperature systems that contain small amounts of melt or fluid depend on the liquid distribution at the grain scale. The presence of a three-dimensional melt network in partially molten rocks and its exact geometry determine permeability and therefore migration and segregation rates of melt in porous flow in the lower crust and upper mantle (McKenzie, 1984; von Bargen and Waff, 1986; Kohlstedt, 1992; Faul, 1997, 2001). At low strain rates, the melt-crystal microstructure is considered to be dominated by surface energy forces (McKenzie, 1984; Kohlstedt, 1992). Static experiments can therefore give insight into natural, slowly deforming partially molten rocks. Many theoretical and experimental studies have been performed for relevant geologic systems; more recently there has been an emphasis on the observation and description of nonequilibrium features that could have important consequences for rock properties (Faul, 1997, 2000; Cmíral et al., 1998; Wark et al., 2003).

For a monomineralic system of equal-sized grains with an isotropic solid-solid and solid-liquid surface energy ($\gamma_{s\text{-}s}$ and $\gamma_{s\text{-}l}$, respectively; Bulau et al., 1979) (Fig. 1A), the ratio of $\gamma_{s\text{-}s}$ to $\gamma_{s\text{-}l}$ determines the dihedral or wetting angle Θ between two crystals and the liquid by the equation

$$2\cos(\Theta/2) = \gamma_{s\text{-}s}/\gamma_{s\text{-}l}. \quad (1)$$

Theoretically, if Θ and the liquid fraction are known, the liquid distribution in this polycrystalline system in thermodynamic equilibrium is fully constrained by the requirement of a constant mean curvature of solid-liquid boundaries (von Bargen and Waff, 1986). Liquid pockets at four-grain junctions are isolated at low-liquid fractions when $\Theta > 60°$ (Fig. 1B). When $\Theta \leq 60°$, a regular three-dimensional network is predicted, regardless of the liquid fraction, with four-grain liquid pockets that are connected by tubes along three-grain junctions (Fig. 1). Boundaries between two grains remain dry as long as $\Theta > 0°$, i.e., $\gamma_{s\text{-}s}/\gamma_{s\text{-}l} < 2$ (equation 1). This theory does not distinguish between melt and fluid and can therefore be applied to both partially molten and aqueous-fluid–bearing systems in textural equilibrium.

To confirm these theoretical predictions and to find the range of wetting angles for significant geologic systems, high-temperature experiments were performed with major rock-forming minerals such as dunite + mafic or ultramafic melt (Hirth and Kohlstedt, 1995; Faul, 1997; Cmíral et al., 1998) or quartz + felsic melt (Jurewicz and Watson, 1984; Laporte, 1994; Laporte and Watson, 1995). In these experiments, Θ is generally well below 60° (e.g., Laporte and Provost, 2000), and the liquid should therefore form a regular three-dimensional network of three-grain tubules. However, in experiments apparent disequilibrium features were described that deviated from the predicted regular melt geometry (Fig. 2): (1) fully wetted grain boundaries; (2) trapped melt lenses between grains; (3) strongly distorted, melt-filled triple junctions; (4) dry triple junctions; and (5) large, multigrain-bounded, melt pools. It has been recognized that variety in grain size and crystal lattice–controlled surface-energy anisotropy modifies the actual liquid distribution in natural aggregates (e.g., Waff and Faul, 1992; Laporte and Watson, 1995; Jung and Waff, 1998; Wark et al., 2003). The frequent observation of straight crystal facets of grains in contact with melt supports the latter explanation for nonequilibrium melt geometries (Waff and Faul, 1992; Hirth and Kohlstedt, 1995; Jung and Waff, 1998; Faul, 1997; Laporte and Provost, 2000). However, features like melt lenses (2) and distorted triple junctions (3) cannot be explained by anisotropy or grain-size variations. For example, the lattice orientation next to a melt lens (2) or a distorted triple junction (3) has to be the same as the lattice orientation next to the dry part of the same grain boundary; therefore, either a fully wetted or a dry grain boundary should be favored, not a melt lens. Although quartz is considered to be more isotropic than olivine, nonequilibrium features 1–5 were observed in quartz + melt systems as well (e.g., Laporte, 1994; Laporte and Provost, 2000).

Nonequigranular grain aggregates in nature are never in static textural equilibrium because of ongoing grain growth (i.e., static grain

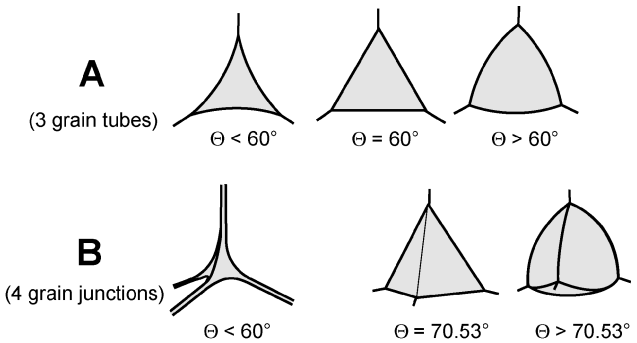

Figure 1. Schematic representation of liquid-phase equilibrium geometry. A: Perpendicular to three-grain tubes. B: Four-grain junctions. Interconnected liquid network only forms at Θ < 60°.

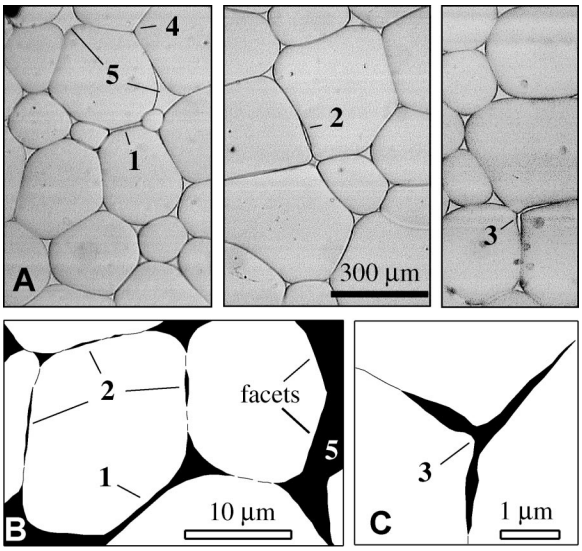

Figure 2. Summary of disequilibrium features. A: Thin sheet of polycrystalline norcamphor with norcamphor-saturated ethanol. See text for experimental details. B: Quartz with water-saturated granitic melt (drawn after Fig. 9, of Laporte and Provost, 2000). C: Olivine with basaltic melt (drawn after Fig. 3B, of Faul, 2000). 1—fully wetted grain boundaries; 2—trapped liquid lenses; 3—distorted triple junctions; 4—dry triple junctions; 5—large liquid patches.

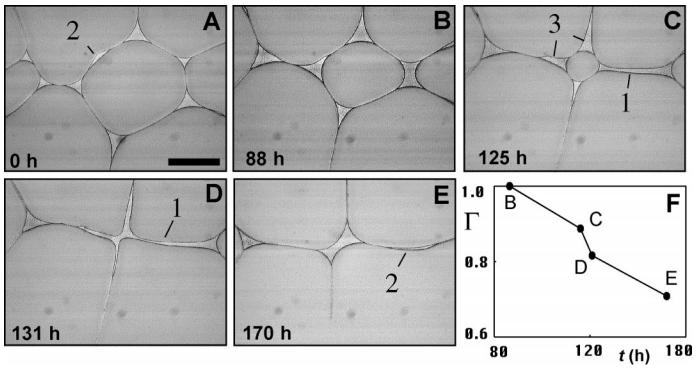

Figure 3. A: Central norcamphor grain surrounded by regular, approximately equal sized triple junctions. B–D: After a neighbor switch (in B), merged fluid patch is pulled into strongly elongate shape by dissolving central grain (in C) until that grain disappears (in D). Initial triple junctions now form strongly distorted cross shape. E: Relaxation of system toward equilibrium fluid distribution. Note remaining fluid lens. F: Normalized total surface energy Γ_{total} vs. time *t* plot. Dots represent conditions in images B–E. Length of scale bar represents 200 μm.

growth) driven by reduction of surface energy (Wearie and Rivier, 1984; Anderson, 1988). How much does this textural nonequilibrium influence melt distribution in natural systems? In order to answer this question we used static in situ analogue experiments of a solid-liquid system. We continuously monitored the textural evolution of the solid-liquid system in order to shed light on the distribution and evolution of disequilibrium structures.

EXPERIMENTS

The system norcamphor + ethanol was used to study the development of solid-liquid systems. Norcamphor is a hexagonal organic crystalline compound that exhibits crystal plastic behavior, analogous to minerals such as quartz, at room temperature (Bons, 1992; Herweg and Handy, 1996). We wedged 20–150-μm-thick samples of norcamphor + norcamphor-saturated ethanol between glass plates. The assembly was placed on a microscope stage and photographed in regular intervals of 5–60 min. At room temperature the aggregate forms a two-dimensional foam texture with smoothly curved grain boundaries between the crystals (Fig. 2A).

The ethanol liquid, which is the melt analogue, is dispersed within the sample, mainly at regular equal-sized triple junctions with concave walls. The solid-liquid wetting angle is ~10°–15°, and the fluid fraction in our experiments ranges between 2% and 8%, remaining constant during an experiment. Norcamphor crystals in contact with liquid show no crystal facets and are therefore considered to have an effectively isotropic $\gamma_{s\text{-}l}$. Varying sample thickness had only minor influence on the microstructural evolution; we therefore conclude that the effect of the glass slides on our results is negligible.

The norcamphor + ethanol aggregate approaches the ideal two-phase model system of an isotropic crystal phase containing a well-wetting ($\Theta < 60°$) fluid or melt phase. The absence of a crystal lattice–controlled anisotropy helps to keep the system simple so that the results are directly comparable to the predictions from equilibrium-based theory. The advantage of using fluid in the experiments, as opposed to using a melt phase, is that all experiments can be performed at room temperature (25 °C) held constant within 1 °C by air conditioning without additional heating. This approach avoids temperature gradients, which can have a strong effect on liquid distribution (Lesher and Walker, 1988). Although a few similar in situ analogue studies involving partial melt or fluid have been performed (Park and Means, 1996; Bauer et al., 2000; Rosenberg and Handy, 2000), no previous experiment was specifically concerned with the effect of static grain growth on melt distribution.

RESULTS

The norcamphor + ethanol aggregate coarsens by static grain growth, in which large, many-sided grains grow at the expense of small, few-sided grains. In areas of the aggregate where the local grain size is uniform, the liquid is distributed as predicted by the equilibrium theory (e.g., Figs. 2A and 3A). However, when neighbor switches occur or small grains disappear, the temporary high curvature of grain boundaries leads to an accelerated grain-boundary velocity, which creates a temporarily distorted liquid distribution. All previously described disequilibrium features (1–5, Fig. 2) are formed in our experiments because of these processes (Figs. 3–6). The experiments show that the features are transitory: a fully wetted grain boundary (1) forms because of a neighbor switch that is finally transformed into a trapped melt lens (2) as the remaining grains merge (Fig. 3). Dry or distorted triple junctions (3, 4) form when a smaller three- or four-sided grain disappears from between the surrounding grains (Figs. 4 and 5). Large fluid patches (5) normally emerge when previous neighbor switches lead grains to disconnect from the surrounding grains and finally dissolve (Fig. 6). None of these features are stable; they revert back toward liquid equilibrium geometry once the small grains have disappeared (Figs. 3E, 4E, and 5E).

Our results show that even in this simple static system, continuous in situ observation is essential to understand the complicated time-dependent processes. Snapshots at any time step, as in high-temperature experiments, would not have revealed the ongoing process but would instead have recorded the disequilibrium features shown in Figure 2.

In order to understand what drives the fluid distribution first out of long-term equilibrium and afterward back toward equilibrium during and after the disappearance of a grain, the local surface energy for the grains in Figures 3–6 was calculated as a function of time. The lengths of solid-solid and solid-liquid boundaries were directly measured from the pictures, $\gamma_{s\text{-}s}$ per unit length was set to unity, and $\gamma_{s\text{-}l}$ was calculated from equation 1, yielding $\gamma_{s\text{-}l} = 0.5043$ per unit length for $\Theta = 15°$.

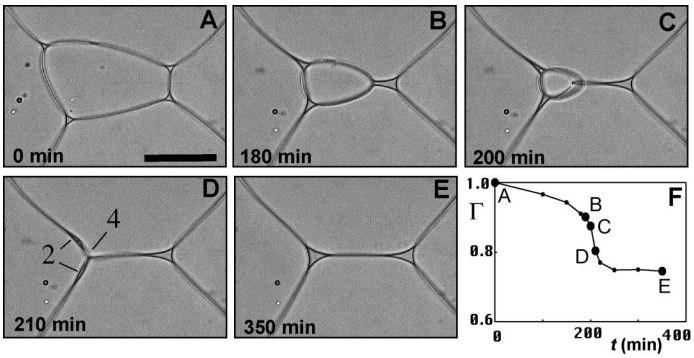

Figure 4. A–C: Four-sided grain is shrinking. After 3 h, neighbor switch occurs, and resulting three-sided grain disappears after 3.5 h. D: Melt-filled triple junctions become elongated and turn into lenticular shape when grain disappears. Note that for short time, result is dry triple junction (4) with two trapped melt lenses (2) nearby. E: Lenses merge and finally form equilibrium melt triangle. F: Normalized Γ_{total} vs. time *t* plot. Large dots represent conditions in images A–E. Length of scale bar represents 100 μm.

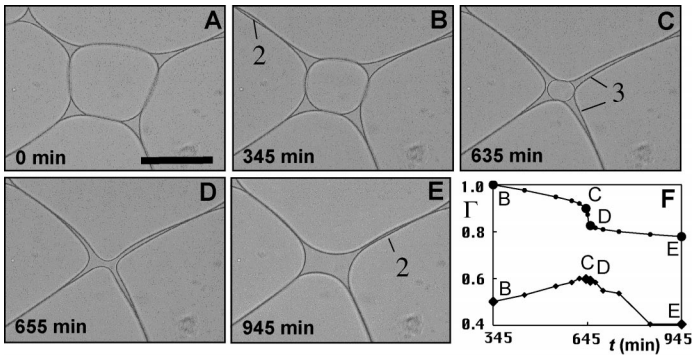

Figure 5. A–C: Disappearance of four-sided grain. D: Melt-filled triple junctions become four-grain junction. Note very low apparent wetting angle (C–D) that evolves during experiment. E: Fluid lens is left even some time after relaxation of system. F: Normalized Γ_{total} vs. time *t* plot (upper curve); $\Gamma_{s\text{-}l}$ vs. *t* plot is given for comparison (lower curve). Large dots represent conditions in images (B–E). Length of scale bar represents 100 μm.

The total solid-solid + solid-liquid surface energy Γ_{total} was normalized to the starting image to track the relative change in time.

The resulting energy vs. time plots show a uniform surface-energy development (Figs. 3F, 4F, 5F, and 6F). Initially, Γ_{total} decreases slowly, then drops very fast during the collapse of the grain. After the grain has disappeared, the surface energy decreases slowly again. The solid-liquid energy ($\Gamma_{s\text{-}l}$) is plotted in Figure 5F for comparison. Although $\Gamma_{s\text{-}l}$ rises because of the formation of a disequilibrium feature (Fig. 5F), the $\Gamma_{s\text{-}s}$ gain by the disappearing grain is more than enough to compensate for this effect. The formation and stability of disequilibrium features can be summarized in two stages: (1) Collapse of small grains leads to fast creation of disequilibrium features owing to a fast drop of Γ_{total}. (2) Solid-liquid surface tension leads to relatively slow healing of disequilibrium features owing to a slower Γ_{total} decrease.

The process of grain coarsening is directly connected to the rate of grain disappearance for a polycrystalline aggregate. Disequilibrium features are therefore continuously created and, because of their slower disappearance, the chance of finding them is high. The resulting geometry can be envisioned as a three-dimensional liquid network consisting of regular triple-junction tubes and quadruple junctions of different sizes modified by continuously changing disequilibrium features (Fig. 2).

DISCUSSION

The similarities between the developing features in the norcamphor experiments and the results of high-temperature experiments are striking (Fig. 2). Static, surface-energy–driven recrystallization is a process that always occurs at elevated temperatures. In fact, to achieve a steady-state microstructure with no inherited effects from the starting powder, most authors of high-temperature experiments took great care to ensure that grain coarsening occurred (e.g., Faul, 1997, 2000). We therefore suggest that our results are directly applicable to quartz-felsic melt aggregates because of the low crystal-lattice anisotropy of quartz. Because of the higher anisotropy of olivine and the regular occurrence of crystal facets, the consequences have to be evaluated carefully for this system. Fully wetted grain boundaries are often approximately parallel to low-index crystallographic planes (crystal facets) in olivine + ultramafic melt systems, according to Jung and Waff (1998). However, they also show many curved crystal surfaces, not crystal facets, that look very similar to our experiments (cf. of Jung and Waff [1998] with our Figs. 3 and 5). Cmíral et al. (1998) found no preference of low-index crystallographic planes for fully wetted grain boundaries in the dunite + melt system. However, Wark et al. (2003) pointed out the problem of interpreting the three-dimensional melt geometry from two-dimensional polished sections. They proposed that most apparent disequilibrium features are explained by sectioning through an ideal melt network modified only by nonequal grain size. Although this sectioning effect might explain some disequilibrium features, the melt lenses (2), distorted triple junctions (3), and large liquid patches (5) with more than four bordering grains are not explained. Note also that our thin-sheet experiments do not have sectioning effects.

We observe a general increase in liquid fraction that is contained in disequilibrium features with overall increasing liquid fraction, as observed by Waff and Faul (1992), Faul (1997), Hirth and Kohlstedt (1995), and Laporte and Provost (2000). However, this result is not due to the higher chance of cutting a four-grain junction, as proposed by Wark et al. (2003), but is rather explained by a lower mean curvature of solid-liquid junctions for higher liquid fractions and, therefore, weaker capillary forces. Disequilibrium features will be more pronounced and last longer when capillary forces are relatively weak. Relatively high capillary forces oppose the formation and stability of disequilibrium features. Therefore, a regular continuous network due to a high mean curvature of solid-liquid junctions is expected for small liquid fractions. In experiments having higher liquid fractions and smaller mean curvatures, more liquid is pooled in disequilibrium features. The effect of developing crystal facets in olivine experiments is difficult to constrain at this stage, but it could help to stabilize the

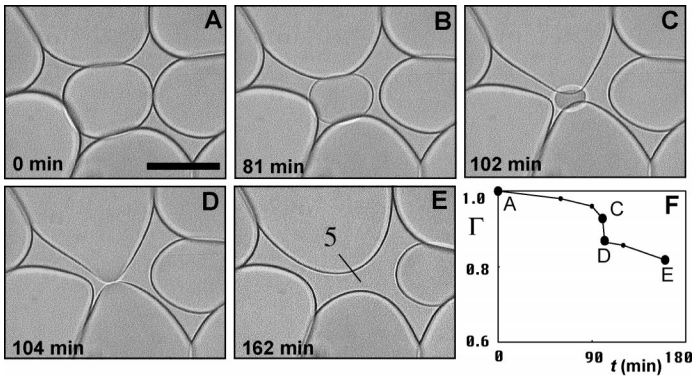

Figure 6. Formation of large liquid patch. A–E: Disappearance of central grain (A–D) leaves large fluid patch bordered by several grains (E). Note solid-solid grain boundary (D) that develops after disappearance of central grain and is separated shortly afterward. F: Normalized Γ_{total} vs. time *t* plot. Large dots represent conditions in images A and C–E. Length of scale bar represents 50 μm.

disequilibrium features such as large melt patches after their initial formation, possibly even at lower liquid fractions.

Two porosity-permeability models for high-temperature liquid-bearing systems have been proposed that lead to strongly contrasting interpretations for general questions of magmatism. The empirical model of Wark and Watson (1998) is based on direct permeability measurements on quartz-fluid aggregates. They reported a continuous porosity-permeability function similar to that of von Bargen and Waff (1986), but about one order of magnitude lower in permeability for a given liquid fraction. Faul (1997, 2001), however, proposed a model based on percolation theory that predicts small liquid fractions ($<2\%$) to be distributed in unconnected lenticular melt pools. If the liquid content is $> 2\%$, the melt pools form a network, resulting in a sharp increase in permeability of approximately four orders of magnitude (Faul, 1997). Wark et al. (2003) questioned the assumptions and methods that led to this threshold model and argued that their continuous model is valid for both olivine-melt systems, as well as for quartz-melt systems.

Our results—a liquid network with few disequilibrium features for small liquid fractions and more disequilibrium features for higher liquid fractions—indicate a more continuous porosity-permeability function such as the empirical function of Wark and Watson (1998) rather than a threshold function like the model of Faul (1997). If liquid geometry in a given system and therefore the system's permeability are strongly dependent on grain coarsening, as we suggest, average grain size, temperature, grain-boundary mobility, second phases, and pinning play an important role in addition to Θ, liquid fraction, and surface-energy anisotropy. Therefore, results of empirical studies have to be considered carefully before they can be applied to nature.

CONCLUSION

We conclude that nonequilibrium melt distributions in partially molten grain aggregates can be explained with the disappearance of small grains due to grain growth. This process may be coupled with and enhanced by crystal lattice–controlled surface-energy anisotropy and formation of crystal facets, as described in olivine + melt systems. Our results support a gradual increase in permeability with liquid fraction (Wark and Watson, 1998) rather than an abrupt increase as in threshold models (Faul, 1997). The aim of this paper is to stress the importance of recrystallization as a major factor for the melt or fluid distribution in high-grade geologic systems.

ACKNOWLEDGMENTS

We thank Jochen Arnold, Jens Becker, Mark Jessell, and Marlina Elburg for many helpful discussions. Walte acknowledges funding by the Deutsche Forschungsgemeinschaft Graduiertenkolleg ''Composition and Evolution of Crust and Mantle.''

REFERENCES CITED

Anderson, M.P., 1988, Simulation of grain growth in two and three dimensions, *in* Hansen, N., et al., eds., Recovery, recrystallization and grain growth: Roskilde, Riso National Laboratory, p. 15–34.

Bauer, P., Rosenberg, C., and Handy, M.R., 2000, ''See-through'' deformation experiments on brittle-viscous norcamphor at controlled temperature, strain rate and applied confining pressure: Journal of Structural Geology, v. 22, p. 281–289.

Bons, P.D., 1992, Experimental deformation of polyphase rock analogues: Geologica Ultraiectina, v. 110, 207 p.

Bulau, J.R., Waff, H.S., and Tyburczy, J.A., 1979, Mechanical and thermodynamical constraints on fluid distribution in partial melts: Journal of Geophysical Research, v. 84, p. 6102–6108.

Cmíral, M., Fitz Gerald, J.D., and Faul, U.H., 1998, A close look at dihedral angles and melt geometry in olivine-basalt aggregates: A TEM study: Contributions to Mineralogy and Petrology, v. 130, p. 336–345.

Faul, U.H., 1997, Permeability of partially molten upper mantle rocks from experiments and percolation theory: Journal of Geophysical Research, v. 102, p. 10,299–10,311.

Faul, U.H., 2000, Constraints on the melt distribution in anisotropic polycrystalline aggregates undergoing grain growth, *in* Bakssarov, N., et al., eds., Physics and chemistry of partially molten rocks: Dordrecht, Kluwer Academic Publications, p. 67–92.

Faul, U.H., 2001, Melt retention and segregation beneath mid-ocean ridges: Nature, v. 410, p. 920–921.

Herweg, M., and Handy, M.R., 1996, The evolution of high-temperature mylonitic microfabrics: Evidence from simple shearing of a quartz analogue (norcamphor): Journal of Structural Geology, v. 18, p. 689–710.

Hirth, G., and Kohlstedt, D.L., 1995, Experimental constraints on the partially molten upper mantle: Deformation in the diffusion creep regime: Journal of Geophysical Research, v. 100, p. 1981–2001.

Jung, H., and Waff, H.S., 1998, Olivine crystallographic control and anisotropic melt distribution in ultramafic partial melts: Geophysical Research Letters, v. 25, p. 2901–2904.

Jurewicz, S.R., and Watson, E.B., 1984, Distribution of partial melt in a felsic system: The importance of surface energy: Contributions to Mineralogy and Petrology, v. 85, p. 25–29.

Kohlstedt, D.L., 1992, Structure, rheology and permeability of partially molten rocks at low melt fractions, *in* Morgen, P.G., et al., eds., Mantle flow and melt generation at mid-ocean ridges: American Geophysical Union Geophysical Monograph 71, p. 103–121.

Laporte, D., 1994, Wetting behavior of partial melt during crustal anatexis: The distribution of hydrous silicic melts in polycrystalline aggregates of quartz: Contributions to Mineralogy and Petrology, v. 116, p. 486–499.

Laporte, D., and Provost, A., 2000, The grain-scale distribution of silicate, carbonate and metallosulfide partial melts: A review of theory and experiments, *in* Bakssarov, N., et al., eds., Physics and chemistry of partially molten rocks: Dordrecht, Kluwer Academic Publications, p. 93–140.

Laporte, D., and Watson, E.B., 1995, Experimental and theoretical constraints on melt distribution in crustal sources: The effect of crystalline anisotropy on melt interconnectivity: Chemical Geology, v. 124, p. 161–184.

Lesher, C.E., and Walker, D., 1988, Cumulate maturation and melt migration in a temperature gradient: Journal of Geophysical Research, v. 93, p. 10,295–10,311.

McKenzie, D., 1984, The generation and compaction of partially molten rock: Journal of Petrology, v. 25, p. 713–765.

Park, Y., and Means, W.D., 1996, Direct observation of deformation processes in crystal mushes: Journal of Structural Geology, v. 18, p. 847–858.

Rosenberg, C.L., and Handy, M.R., 2000, Syntectonic melt pathways during simple shearing of a partially molten rock analogue (norcamphor-benzamide): Journal of Geophysical Research, v. 105, p. 3135–3149.

von Bargen, N., and Waff, H., 1986, Permeabilities, interfacial areas and curvatures of partially molten systems: Results of numerical computations of equilibrium microstructures: Journal of Geophysical Research, v. 91, p. 9261–9276.

Waff, H., and Faul, U.H., 1992, Effects of crystalline anisotropy on fluid distribution in ultramafic partial melts: Journal of Geophysical Research, v. 97, p. 9003–9014.

Wark, D.A., and Watson, E.B., 1998, Grain-scale permeability of texturally equilibrated, monomineralic rocks: Earth and Planetary Science Letters, v. 164, p. 591–605.

Wark, D.A., Williams, C.A., Watson, E.B., and Price, J.D., 2003, Reassessment of pore shapes in microstructurally equilibrated rocks, with implications for permeability of the upper mantle: Journal of Geophysical Research, v. 108, no. 2050, DOI 10.1029/2001JB001575.

Wearie, D., and Rivier, N., 1984, Soap, cells and statistics—Random patterns in two dimensions: Contemporary Physics, v. 25, p. 59–99.

Manuscript received 9 May 2003
Revised manuscript received 5 August 2003
Manuscript accepted 5 August 2003

Printed in USA